PROBABILISTIC TRACKING OF VIRUS PARTICLES IN FLUORESCENCE MICROSCOPY IMAGES

W. J. Godinez[1], M. Lampe[2], S. Wörz[1], B. Müller[2], R. Eils[1], and K. Rohr[1]

[1]University of Heidelberg, BIOQUANT, IPMB, and DKFZ Heidelberg,
Dept. Bioinformatics and Functional Genomics, Biomedical Computer Vision Group,
Im Neuenheimer Feld 267, 69120 Heidelberg, Germany,
[2]University of Heidelberg, Dept. of Virology, Im Neuenheimer Feld 324, 69120 Heidelberg, Germany

ABSTRACT

Fluorescence time-lapse microscopy is a powerful technique for observing the spatial-temporal behavior of viruses. To quantitatively analyze the exhibited dynamical relationships, tracking of viruses over time is required. We have developed probabilistic approaches based on particle filters for tracking multiple virus particles in time-lapse fluorescence microscopy images. We employ a mixture of particle filters as well as independent particle filters. For the latter, we have developed a penalization strategy to maintain the identity of the tracked objects in cases where objects are in close proximity. We have also extended the approaches for tracking in multi-channel microscopy image sequences. The approaches have been evaluated based on synthetic images and the performance has been quantified. We have also successfully applied the approaches to real microscopy images of HIV-1 particles and have compared the tracking results with ground truth from manual tracking.

Index Terms— Biomedical imaging, microscopy image sequences, tracking virus particles.

1. INTRODUCTION

The aim of our work is to study the dynamic behavior of the human immunodeficiency virus (HIV) based on live cell microscopy using fluorescently labeled virus particles. Tracking single virus particles yields quantitative information that contributes to the understanding of viral processes (e.g., cell entry). To obtain statistically sound conclusions, many individual particles must be tracked. Automatic tracking techniques are required to analyze a large number of image sequences. However, tracking virus particles is challenging. Problems are due to the small size of viruses as well as their complex motion behavior. In addition, one has to cope with the large number of virus particles, the relatively high level of cellular autofluorescence, as well as a relatively low signal-to-noise ratio (SNR).

In previous work on *virus tracking*, a *deterministic* two-step paradigm encompassing virus localization and motion correspondence has been typically employed. For virus localization, most approaches employ a maximum intensity search strategy, where intensity maxima are associated with candidate virus particles (e.g., [1]). Model fitting may be employed to enhance the localization accuracy (e.g., [2]). For motion correspondence, approaches that consider the motion of all viruses via graph-theoretical algorithms have been used (e.g., [3]). In contrast to the deterministic schemes, *probabilistic* approaches are generally characterized by the inclusion of a spatial-temporal filter. An approach using a pool of Kalman filters has been presented in [4]. However, the steps of object localization and spatial-temporal filtering are uncoupled. This entails that temporal information is not used for object localization, and analogously image information is not directly used by the filter to estimate the position of an object. In contrast to the Kalman filter, the particle filter, which has been introduced to the field of computer vision in [5], exploits more effectively the image and temporal information encoded in an image sequence. An approach using a mixture of particle filters for virus tracking has been described in [6]. There, however, only a fixed number of objects could be tracked. Generally, in real applications, the number of objects changes over time (e.g., objects enter the field of view or visible objects disappear). For use of a mixture of particle filters in a different application, namely tracking of microtubules, we refer to [7].

In this contribution, we describe probabilistic approaches based on particle filters for tracking multiple viruses in fluorescence microscopy time-lapse images. Whereas in our earlier work we used a *mixture of particle filters* (MPF) [6], we here introduce an approach using *independent particle filters* (IPF). In contrast to the approach using MPF, the approach using IPF can track a variable and unknown number of objects. A problem with standard IPF is that the independent filters may attach to the same object. We address this problem via a novel penalization mechanism based on a deterministic motion correspondence algorithm. The investigated approaches are fully automatic and have been successfully applied to a large number of synthetic image sequences displaying virus-like objects as well as to relatively long real microscopy im-

age sequences (e.g., more than 200 frames) displaying HIV-1 particles.

2. TRACKING OF MULTIPLE VIRUS PARTICLES

In our approaches, tracking is formulated as a Bayesian sequential estimation problem. Within a *one-body state space*, it is assumed that a virus particle is represented by a state vector $\mathbf{x}_t$ and that a noisy measurement $\mathbf{y}_t$ reflects the true state of $\mathbf{x}_t$. At time step t, the aim is to estimate the state $\mathbf{x}_t$ of a virus given a sequence of measurements $\mathbf{y}_{1:t}$. By modeling the temporal evolution using a *dynamical model* $p(\mathbf{x}_t|\mathbf{x}_{t-1})$ and incorporating measurements derived from the images via a *measurement model* $p(\mathbf{y}_t|\mathbf{x}_t)$, a Bayesian filter estimates the *posterior* distribution $p(\mathbf{x}_t|\mathbf{y}_{1:t})$ via stochastic propagation and Bayes' theorem:

$$p(\mathbf{x}_t|\mathbf{y}_{1:t}) \propto p(\mathbf{y}_t|\mathbf{x}_t) \int p(\mathbf{x}_t|\mathbf{x}_{t-1})\, p(\mathbf{x}_{t-1}|\mathbf{y}_{1:t-1})\, d\mathbf{x}_{t-1}.$$

An estimate of $\mathbf{x}_t$ can be obtained from the posterior $p(\mathbf{x}_t|\mathbf{y}_{1:t})$, which, in our case, is estimated using a particle filter. The idea of this algorithm is to approximate the posterior via a set $\{\mathbf{x}_t^i; w_t^i\}_{i=1}^{N_s}$ of N_s random samples $\mathbf{x}_t^i$ (the 'particles') that are associated with importance weights w_t^i. Below, we briefly describe the tracking approach based on a mixture of particle filters (MPF) and then we present our approach based on independent particle filters (IPF).

2.1. Mixture of Particle Filters (MPF)

In the case of tracking multiple objects that have a similar appearance, multiple modes arise in the posterior distribution, where each mode corresponds to one object. Although a standard particle filter is in principle able to handle such a distribution, it is well-known that this filter cannot maintain the multimodality over several time steps [5],[8]. To address this problem, one may model the posterior $p(\mathbf{x}_t|\mathbf{y}_{1:t})$ as a non-parametric *M*-component *mixture model*:

$$p(\mathbf{x}_t|\mathbf{y}_{1:t}) = \sum_{m=1}^{M} \pi_{m,t}\, p_m(\mathbf{x}_t|\mathbf{y}_{1:t}),$$

where $\pi_{m,t}$ denotes the component weight of the *m-th* component [8]. Each *m-th* component is now approximated using a set of particles $\{\mathbf{x}_t^i; w_t^i\}_{i\in\tau_m}$, where τ_m is the set of indices indicating which particles belong to component m, and particles are allocated to each component using a clustering mechanism. Note that $\sum_{m=1}^{M} |\tau_m| = N_s$, where $|\cdot|$ denotes the set size operator; note also that $|\tau_m|$ may vary for each component. If tracking a variable and unknown number of objects, the performance of this approach deteriorates as the number of objects increases, since the number of particles N_s that approximates the mixture model remains constant, i.e., fewer particles are allocated to each *m-th* component, thereby attaining a lower estimation accuracy.

2.2. Independent Particle Filters (IPF)

Alternatively, one may track multiple objects by instantiating one *independent particle filter* per object. In this case, each filter uses an independent set of particles of size N_s. In contrast to the mixture approach, the estimation accuracy does not deteriorate as the number of objects increases, since each filter uses an independent set of particles of size N_s. Failures arise when objects are in close proximity, since the filters converge towards the object with the best likelihood $p(\mathbf{y}_t|\mathbf{x}_t)$. Approaches to address this problem have been proposed by [9],[10]. In [9], an exclusion mechanism based on a magnetic potential model has been proposed for tracking human faces. In [10], the mean-shift algorithm has been used for deterministically biasing the particles; this approach has been applied for tracking hockey players. The former approach prevents objects from merging, which is not desirable in our application, while the latter approach might yield an incorrect offset due to the close proximity of multiple objects with a similar appearance.

In contrast to [9],[10], we propose a novel penalization strategy that is based on both probabilistic and deterministic information, and which does not necessarily preclude objects from merging. Our approach comprises three steps: first, the approach determines objects that are in close proximity. This reduces to finding cliques in an undirected graph $\Gamma = (V, E)$, where a vertex v_i is defined by the filtered position estimate of object i, and an edge $e = \{v_i, v_j\}$ is said to join vertices v_i and v_j if the Euclidean distance between the positions of the two objects is below a predefined value. The second step determines the most plausible position $\hat{\mathbf{x}}_t$ for each object in each clique. For this purpose, modes are sought in the probability density function that is induced by merging all particles of all filters of one clique: given k objects, such a distribution exhibits k modes. In some cases, k modes might not be obtainable, for instance, if objects are too close to one another. The assignment of modes to objects is carried out via a deterministic motion correspondence algorithm, namely a global nearest neighbor approach [1]. If no mode (i.e., no most plausible position) is assigned to an object, this object is not further considered in the penalization scheme. This entails that the penalization scheme may allow filters to coalesce for a while. In the third step, the weights of those misleading particles that are relatively distant to the most plausible position $\hat{\mathbf{x}}_t$ of an object are assigned lower values via a Gaussian function centered at $\hat{\mathbf{x}}_t$ with a standard deviation $\sigma_{penalize}$. Given the lower weights, the resampling step of the particle filter may discard the misleading particles, thereby preventing filters from coalescing.

2.3. Model of Virus Particles

We model the intensity distribution of each virus particle by a 2D Gaussian function, which is parametrized by the position of the virus, the peak intensity, and the standard deviation;

these parameters constitute the state $\mathbf{x}$. For the dynamical model $p(\mathbf{x}_t|\mathbf{x}_{t-1})$, we assume that the components of $\mathbf{x}$ follow independent Gaussian random walk dynamics. The measurement model $p(\mathbf{y}_t|\mathbf{x}_t)$ measures the probability that the predicted state $\mathbf{x}_t$ generated a Gaussian intensity distribution in the image. In our application, the microscopy image sequences comprise two channels ('red' and 'green' channel). To analyze two-channel image sequences we suggest the following extension of the measurement model:

$$p_{2-channel}(\mathbf{y}|\mathbf{x}) \propto \exp\left(-\frac{D(\mathbf{y}_r, \mathbf{g}(\mathbf{x}))^2 + D(\mathbf{y}_g, \mathbf{g}(\mathbf{x}))^2}{2\sigma_n^2}\right),$$

where $\mathbf{y}_r$ and $\mathbf{y}_g$ are the image intensities in the red and green channels, respectively, $\mathbf{g}(\mathbf{x})$ is a synthetic image generated using the 2D Gaussian appearance model, and $D(\cdot)$ is a distance function (e.g., Euclidean distance); the parameter σ_n regulates the expected degree of noise.

3. EXPERIMENTAL RESULTS

We have applied our approaches to synthetic as well as real microscopy image sequences. To automatically detect virus particles, we employ either the spot-enhancing filter (SEF) [11] or 2D Gaussian fitting (GaussFit) and combine them with the particle filter approaches. The approaches using a mixture of particle filters (MPF) can only track objects that are visible at time step $t = 0$, while those using independent particle filters (IPF) can track objects that enter the field of view at any time step. For motion correspondence between the detected particles and the independent filters we employ a global nearest neighbor approach. To measure the performance, we use the tracking accuracy defined as $P_{track} = \frac{n_{track,correct}}{n_{track,total}}$, which reflects the ratio between the number of correctly computed trajectories $n_{track,correct}$ and the number of true trajectories $n_{track,total}$. The value for $n_{track,correct}$ is computed as the weighted sum of the percentage of tracked time steps $r_{tracked,i}$ for each *i-th* true trajectory: $n_{track,correct} = \sum_{i=1}^{n_{track,total}} w_i r_{tracked,i}$, where the weight w_i is given by a Gaussian function, which takes as its argument the number of correctly computed trajectories $n_{track,i}$. The weighting scheme is introduced to penalize computed trajectories that are broken. Note that $P_{track} \in [0, 1]$.

We first validated the approaches based on a large number of synthetic image sequences. Here, we describe the experimental results obtained for one illustrative image sequence. This sequence consists of 100 images (256×256 pixels, 16-bit) displaying 20 synthetic Gaussian-like particles, which enter or leave the field of view at certain time steps. The SNR level is 4.55 and the noise model is assumed to be Poisson distributed. The quantitative experimental results are as follows: SEF&MPF achieves 79.28%, GaussFit&MPF attains 80.00%, SEF&IPF yields 85.65%, and GaussFit&IPF achieves 90.13%. Thus the IPF approaches yield superior results.

Table 1: Description of real microscopy image sequences.

	Dimensions	No. of time steps	No. of objects
Seq. 1	256×256	250	23
Seq. 2	512×512	200	15
Seq. 3	512×512	400	43
Seq. 4	256×256	150	21
Seq. 5	512×512	400	24

Table 2: Tracking performance P_{track} [%] for real microscopy image sequences.

	SEF& MPF	GaussFit& MPF	SEF& IPF	GaussFit& IPF
Seq. 1	84.82	81.95	86.73	82.61
Seq. 2	84.64	85.64	93.54	93.54
Seq. 3	50.62	49.04	74.64	67.76
Seq. 4	28.52	23.81	71.10	83.39
Seq. 5	48.51	52.61	73.55	76.89

We also validated the algorithms using real microscopy image sequences. In these sequences, fluorescently labeled HIV-1 particles were imaged using a fluorescence wide-field microscope. Fluorophores were excited with their respective excitation wavelengths and movies were recorded with a frequency of 10Hz [12]. Ground truth for the virus positions was obtained by manual tracking using the commercial software MetaMorph. The quantitative experimental results for five sequences are presented in Table 2. Each sequence consists of 150 up to 400 frames (see Table 1). Analogously to the experiments using synthetic data, it turns out that the approaches using IPF yield a higher tracking accuracy than the approaches using MPF.

Sample images of tracking results for a section of the real sequence "Seq. 4" are shown in Fig. 1. Besides the results for the MPF and IPF, we also show the results obtained with IPF *without* employing a strategy to prevent filter coalescence (standard IPF). In this case, it can be seen that the filters attach to the objects with the best likelihoods, resulting in a fewer number of tracked objects. In contrast, our extended IPF approach, via the proposed penalization scheme, maintains the identities of the virus particles, in particular, of those that are in close proximity (e.g., virus particles '2' and '4' as well as '7' and '8' shown in the results for IPF).

We have also applied our approaches to both channels of real microscopy image sequences, where the first channel corresponds to the red fluorescent protein (RFP) signal while the second channel corresponds to the green fluorescent protein (GFP) signal. Generally, virus particles are visible in both channels. In some cases, however, a particle disappears from one channel, while remaining visible in the other channel. In Fig. 2, we show the tracking results for an ROI (76×87 pixels)

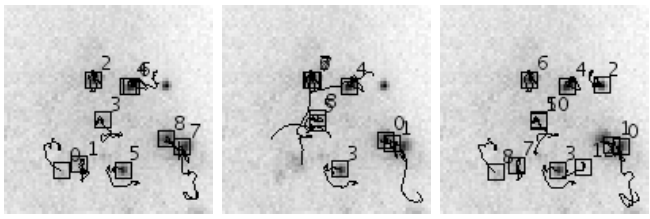

MPF, $t = 74$ Standard IPF, $t = 74$ IPF, $t = 74$

Figure 1: Tracking results for a section of the real image sequence "Seq. 4" for time step $t = 74$: mixture of particle filters (MPF) (left), standard independent particle filters (Standard IPF) (center) and independent particle filters in combination with our penalization strategy (IPF) (right).

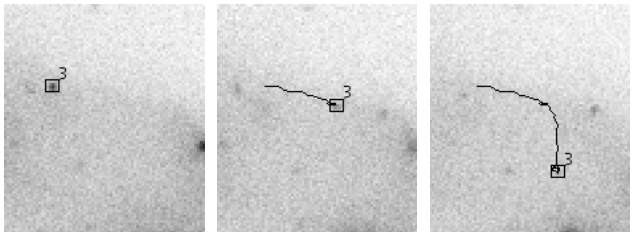

IPF, $t = 0$ (RFP) IPF, $t = 50$ (RFP) IPF, $t = 100$ (RFP)

Figure 2: Tracking results for the real two-channel image sequence "Seq. 2". The results for GaussFit&IPF using both channels are overlaid on the images from the RFP channel; only the trajectory for the considered object is displayed.

from "Seq. 2" as an illustrative example. The results demonstrate that by employing the information from both channels, our approach (in this case GaussFit&IPF) can retrieve the entire trajectory of the virus particle in the middle of the depicted section, which disappears at time step $t = 68$ from the RFP channel.

4. DISCUSSION

We have presented probabilistic approaches based on particle filters for tracking multiple viruses in microscopy image sequences. In particular, we have introduced an approach using independent particle filters in conjunction with a penalization scheme to maintain the identity of objects in close proximity. Our quantitative experimental results based on synthetic and relatively long real microscopy image sequences show that the new approach is superior to a previously developed approach based on a mixture of particle filters. In addition, we described an extension of our approaches for analyzing two-channel image sequences. This allows studying events of biological interest, e.g., the colocalization of proteins.

Acknowledgements

Support of the BMBF (FORSYS) project VIROQUANT is gratefully acknowledged.

5. REFERENCES

[1] I. F. Sbalzarini and P. Koumoutsakos, "Feature point tracking and trajectory analysis for video imaging in cell biology," *J. Struct. Biol.*, vol. 151, no. 2, pp. 182–195, 2005.

[2] G. Seisenberger, M. U. Ried, T. Endress, H. Buning, M. Hallek, and C. Bräuchle, "Real-time single-molecule imaging of the infection pathway of an adeno-associated virus," *Science*, vol. 294, no. 5548, pp. 1929–1932, 2001.

[3] G. J. Schutz, H. Schindler, and T. Schmidt, "Single-molecule microscopy on model membranes reveals anomalous diffusion," *Biophys. J.*, vol. 73, no. 2, pp. 1073–1080, 1997.

[4] N. Arhel, A. Genovesio, K. Kim, S. Miko, E. Perret, J. Olivo-Marin, S. Shorte, and P. Charneau, "Quantitative four-dimensional tracking of cytoplasmic and nuclear HIV-1 complexes," *Nat. Methods*, vol. 3, no. 10, pp. 817–824, 2006.

[5] M. Isard and A. Blake, "CONDENSATION – conditional density propagation for visual tracking," *International Journal of Computer Vision*, vol. 29, no. 1, pp. 5–28, 1998.

[6] W. J. Godinez, M. Lampe, S. Wörz, B. Müller, R. Eils, and K. Rohr, "Tracking of virus particles in time-lapse fluorescence microscopy image sequences," in *Proc. ISBI'07*, Arlington, VA, USA, April 2007, IEEE, pp. 256–259.

[7] I. Smal, W. Niessen, and E. Meijering, "Advanced particle filtering for multiple object tracking in dynamic fluorescence microscopy images," in *Proc. ISBI'07*, Arlington, VA, USA, April 2007, IEEE, pp. 1048–1051.

[8] J. Vermaak, A. Doucet, and P. Pérez, "Maintaining multi-modality through mixture tracking," in *Proc. ICCV'03*, Nice, France, October 2003, IEEE, pp. 1110–1116.

[9] W. Qu, D. Schonfeld, and M. Mohamed, "Real-time interactively distributed multi-object tracking using a magnetic-inertia potential model," in *Proc. ICCV'05*, Beijing, China, October 2005, IEEE, vol. 1, pp. 535–540.

[10] Y. Cai, N. de Freitas, and J. J. Little, "Robust visual tracking for multiple targets," in *Proc. ECCV'06*, Graz, Austria, May 2006, pp. 107–118.

[11] D. Sage, F. R. Neumann, F. Hediger, S. M. Gasser, and M. Unser, "Automatic tracking of individual fluorescence particles: Application to the study of chromosome dynamics," *IEEE Trans. Image Process.*, vol. 14, no. 9, pp. 1372–1382, 2005.

[12] M. Lampe, J. A. G. Briggs, T. Endress, B. Glass, S. Riegelsberger, H.-G. Kräusslich, D. C. Lamb, C. Bräuchle, and B. Müller, "Double-labelled HIV-1 particles for study of virus-cell interaction," *Virology*, vol. 360, no. 1, pp. 92–104, 2007.